applied sciences

MDPI

Article

Tailoring of Highly Intense THz Radiation Through High Brightness Electron Beams Longitudinal Manipulation

Flavio Giorgianni [1,*], Maria Pia Anania [2], Marco Bellaveglia [2], Angelo Biagioni [2], Enrica Chiadroni [2], Alessandro Cianchi [3], Maddalena Daniele [2], Mario Del Franco [2], Domenico Di Giovenale [2], Giampiero Di Pirro [2], Massimo Ferrario [2], Stefano Lupi [1], Andrea Mostacci [4], Massimo Petrarca [4], Stefano Pioli [2], Riccardo Pompili [2], Vladimir Shpakov [2], Cristina Vaccarezza [2] and Fabio Villa [2]

1 National Institute of Nuclear Physics (INFN) and Department of Physics, "Sapienza" University of Rome, Piazzale A. Moro 2, I-00185 Rome, Italy; stefano.lupi@roma1.infn.it

2 Frascati National Laboratories, INFN, via Enrico Fermi 40, I-00044 Frascati, Italy; maria.pia.anania@lnf.infn.it (M.P.A.); marco.bellaveglia@lnf.infn.it (M.B.); angelo.biagioni@lnf.infn.it (A.B.); enrica.chiadroni@lnf.infn.it (E.C.); maddalena.daniele@lnf.infn.it (M.D.); mario.delfranco@lnf.infn.it (M.D.F.); domenico.digiovenale@lnf.infn.it (D.D.G.); giampiero.dipirro@lnf.infn.it (G.D.P.); massimo.ferrario@lnf.infn.it (M.F.); stefano.pioli@lnf.infn.it (S.P.); riccardo.pompili@lnf.infn.it (R.P.); vladimir.shpakov@lnf.infn.it (V.S.); cristina.vaccarezza@lnf.infn.it (C.V.); fabio.villa@lnf.infn.it (F.V.)

3 INFN and Department of Physics, "Tor Vergata" University, via della Ricerca Scientifica 1, 00133 Rome, Italy; alessandro.cianchi@roma2.infn.it

4 INFN and Department of Basic and Applied Sciences for Engineering (SBAI), "Sapienza" University of Rome, Via A. Scarpa 14, 00161 Rome, Italy; andrea.mostacci@uniroma1.it (A.M.); massimo.petrarca@uniroma1.it (M.P.)

* Correspondence: flavio.giorgianni@roma1.infn.it; Tel.: +39-06-4991-3485

Academic Editor: Christoph Hauri
Received: 4 November 2015; Accepted: 3 February 2016; Published: 18 February 2016

Abstract: The ultra-short electron beams, produced through the velocity bunching compression technique at the SPARC_LAB test Facility (Frascati, Italy), are used to produce Coherent Transition Radiation in the terahertz (THz) range. This paper reports on the main features of this THz source, which have a spectral coverage up to 5 THz, a pulse duration down to 100 fs, and an energy per pulse on the order of tens of μJ. These figures of merits open the possibility to apply this source for nonlinear and THz pump-probe experiments in Solid-State Physics and material science.

Keywords: terahertz; terahertz source; electron beams; ultrashort pulses

1. Introduction

Terahertz radiation (30 GHz–15 THz, 20–1000 μm; 1–60 meV) is a portion of the electromagnetic (e.m.) spectrum, which lies in the gap between Microwave and Infrared. THz-based technologies and research applications have seen a rapid increment in the last years due to the development of new radiation sources based both on femtosecond lasers and sub-picosecond electron bunches [1,2].

Intense single cycle pulses are increasingly used to explore the nonlinear light-matter interaction at THz frequency spanning from a coherent control of quantum states to induce and externally modify chemical and/or biological processes [3,4]. Recently, laser-based sources have reached pulse energies on the level of tens of μJ by optical rectification of mJ laser pulses [2,5,6]. However, photon down-conversion process suffers of limitations to generate high power THz pulses, like the damage threshold of the nonlinear crystals and saturation conversion efficiency. Accelerator-based sources

may provide instead a viable way to produce highly intense THz pulses without the limitations of optical conversion processes.

At the SPARC_LAB test facility [7], highly intense broadband THz radiation is routinely produced as Coherent Transition Radiation (CTR) emitted by ultra-short (∼100 fs) high-brightness electron bunches [8]. These bunches are produced through the velocity bunching compression technique [9–11]. The main feature of this source relies on the possibility of generating an e.m. spectrum in the THz range of different bandwidth, centered at different frequencies spanning from 0.5 up to 5 THz, by simply acting on laser pulse shaping and longitudinal phase space manipulation techniques. This method makes the SPARC_LAB THz source flexible, allowing both broadband and narroband THz generation, taking advantage from the laser comb technique integrated in the velocity bunching regime [12]. This versatility is not possible in both undulator-based and dielectric waveguide THz sources [13,14], where the broadband emission cannot be achieved. In addition, unlike other ways of bunch train generation, for instance chirped-pulse beating [15] and dispersive mask techniques [16], the laser comb scheme permits a full control of both the temporal bunch inter-distance and the amplitude pulse shape. In particular, a custom train of more than 100 pC charge/bunch can be generated at the cathode and transported with no losses up to the THz station. Therefore, in case of a 4 bunches train with 100 pC/bunch, the THz radiation energy per pulse would be equivalent to that generated by a 400 pC single bunch. So, our laser technique allows to control the laser pulse amplitude, *i.e.*, bunch charge, and the temporal delay of each pulse with respect to the other directly at the cathode, resulting in a customized THz emission spectrum.

In this paper, we will resume the main results achieved at SPARC_LAB in the generation of CTR-THz radiation, due to the peculiar possibility of longitudinally manipulating ultra-short (sub-ps) high-brightness electron beams.

The measured THz figures of merit render the SPARC_LAB source one of the most performant sources worldwide for nonlinear and pump-probe THz spectroscopy. From this point of view, the opportunity of proper tailoring the THz spectral shape by the bunch train is very compelling because it would allow to selectively pump excitations in a condensed matter systems [17,18]. Furthermore, we show that the characterization of coherent THz radiation spectrum is a valid and useful tool for longitudinal diagnostics of exotic sub-ps electron beams in new Free-Electron Laser sources [19] and for future plasma accelerated femtosecond scale, pC electron bunches [20].

2. Theoretical Background

The fundamental mechanism of emission considered here is the Transition Radiation (TR) effect as generated when a relativistic charged particle crosses the boundary between two media of different dielectric properties, e.g., a vacuum-metal screen interface [21]. TR originates from the time varying currents induced, on the target surface, by the electromagnetic field of the traveling charges, due to optical inhomogeneities in the space. Assuming a perfectly conducting flat screen with rectangular $h \times l$ dimensions, the spectral and spatial intensity distribution from a single electron $\frac{d^2 I_{sp}}{d\omega d\Omega}$ is well described by the virtual-photon method [22]:

$$\frac{d^2 I_{sp}}{d\omega d\Omega} = \frac{1}{4\pi\epsilon_0}\frac{e^2\omega^2}{4\pi^2 c}\left(|E_x|^2 + |E_y|^2\right), \tag{1}$$

where $E_{x(y)}$ is the horizontal (vertical) components of the emitted field:

$$E_{x(y)}(k_x, k_y) = \frac{4ek}{2\pi^2 vR}\int_{-\infty}^{\infty}\int_{-\infty}^{\infty} d\kappa_x d\kappa_y \frac{\kappa_{x(y)}}{\kappa_x^2 + \kappa_y^2 + \alpha^2}\frac{sin(\frac{l}{2}(k_x + \kappa_x)}{k_x - \kappa_x} \left\{\frac{sin[\frac{l}{2}(k_y - \kappa_y)]}{k_y - \kappa_y} - \frac{sin[\frac{h}{2}(k_y - \kappa_y)]}{k_y - \kappa_y}\right\}, \tag{2}$$

with $\alpha = \frac{\omega}{\beta c \gamma}$, R is the distance between the center of screen and the observation point, while k_x and k_y are the projections of the light wavevector $\vec{k}$ on the x-y plane.

When considering a bunch of spatially distributed N charged particles, each particle emits TR on the screen with the same intensity, while the relative phase difference depends on the position within the bunch and on the radiation emission direction. The total emitted intensity can be written as

$$\frac{d^2I}{d\omega d\Omega} = \frac{d^2I_{sp}}{d\omega d\Omega}[N + N(N-1)F(\omega)] \tag{3}$$

where $F(\omega)$ is the longitudinal form factor of the bunch which is the squared of Fourier transform of the longitudinal charge distribution. The total emitted energy $\frac{d^2I}{d\omega d\Omega}$ shows two different regimes: (i) at wavelengths $\lambda = 2\pi c/\omega$ smaller than the longitudinal electron bunch size, typically tens or few hundreds of microns, $F(\lambda)$ tends to 0 and the spectrum is dominated by incoherent emission (whose intensity is proportional to the number of particles N in the bunch); (ii) at longer wavelengths, with respect to the bunch length, emission starts to be coherent (corresponding to an intensity proportional to N^2) because each electron emits in phase and the amplitudes add constructively: $F(\lambda)$ tends to 1. For sub-ps electron beams the coherent regime occurs at THz range. From this point of view, the N^2 dependency of coherent radiation results in a huge intensity gain with respect to most existing THz sources.

For a single gaussian-shaped electron beam, shown in Figure 1a, the calculated spectrum combining Equations (2) and (3) is depicted in Figure 1b by a dotted red line. As one can observe, a single electron bunch with a 100 fs (RMS) pulse duration generates a broadband THz spectrum up to 6 THz. However, the emitted spectrum suffers of a low frequency cut-off due to finite screen dimension [22], which occurs when natural extent of the particle field $\gamma\lambda/2\pi$ exceeds the screen size. In particular, as observed in Figure 1b, for a 30 × 30 mm the low frequency cut-off is around 0.3 THz.

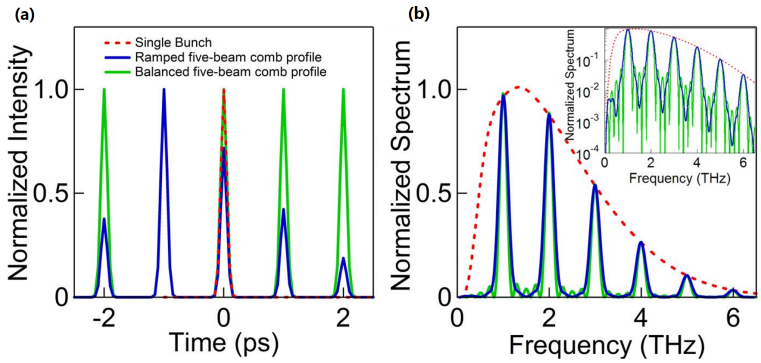

Figure 1. Numerical calculation of terahertz (THz) generation by a train of ps-spaced bunches: (**a**) Bunch profile: single bunch (red dotted line), five-bunch comb beam (green curve), five-bunch comb beam with ramp charge distribution (blue curve). The bunch length is 100 fs, while the comb inter-distance is 1 ps equal to a repetition rate of 1 THz; (**b**) Corresponding generated spectra. Inset: spectra generated in logarithmic scale.

If a longitudinally modulated electron beam, called comb beam, with THz repetition rate is transported to the TR screen, narrowband emission occurs at discrete frequencies multiple to the inverse of the pulse train inter-distance. For example, the spectrum of a five-comb bunches with 1 THz repetition rate, as that shown in Figure 1a, has a comb shape in which peaks have an interdistance of 1 THz and whose intensity envelope is the same as if all the electrons were confined in the single sub-pulse.

The spectrum generated by a uniform bunch train shows also a set of secondary peaks, whose intensity in the calculated case (bunch duration of 100 fs and comb repetition rate 1 THz) is ∼5% respect to the intensity of the main peaks. This effect could reduce the visibility of main narrow peaks.

A possibility to increase the visibility of the main peaks consists of giving a charge modulation to the bunches, for example a ramp comb beam, as shown in Figure 1a by a blue line. Indeed, the spectrum generated by a ramp comb train shows a reduction of the background modulation of about a factor of 50 with respect to the one generated by a balanced train of bunches, as shown in the inset of Figure 1b.

3. THz Source Experimental Layout

The SPARC_LAB photoinjector (INFN-LNF, Frascati, Italy), which consists in a RF Gun and 3 S-Band travelling wave accelerating sections, is able to provide high brightness electron beams boosted up to 170 MeV at 10 Hz repetition rate. A schematic layout is shown in Figure 2a.

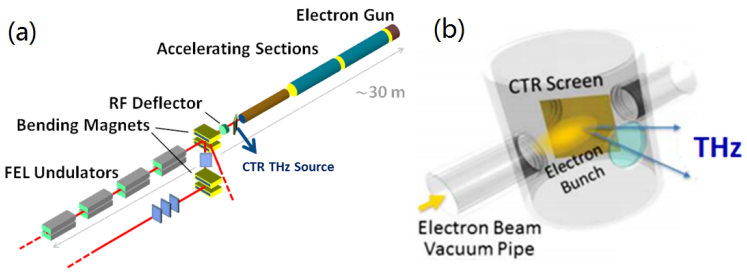

Figure 2. (**a**) Simplified cartoon of SPARC_LAB ; (**b**) Experimental layout of the THz source chamber placed at the end of the linac.

Ultra-short electron bunches, mandatory for the generation of broadband high intense THz pulses, are generated at SPARC_LAB through RF compression in the so-called velocity bunching (VB) regime. The electron beam is injected in the first accelerating section at the zero crossing RF field phase. Since the beam is slightly slower than the phase velocity of the RF wave, a longitudinal phase space rotation occurs, based on a time-velocity chirp in the electron bunch, for which electrons in the tail are faster than those in the bunch head. As consequence, the electron beam slips back to phases where the field is accelerating, but it is simultaneously chirped and compressed. The so generated ultra-short, ∼100 fs, and highly charged, up to ∼600 pC, electron bunches reach the THz station placed at the end of the linac, as reported in Figure 2a. A diagnostic transfer line, right after the THz station, and equipped with a RF deflecting cavity (RFD), quadrupoles and a dipole magnet, allows a full 6D characterization of the electron beam.

Figure 2b reports sketch of the THz source chamber. In our case, TR is produced on a 30 × 30 mm aluminum coated silicon plate placed at 45° with respect to the electron beam direction, which both generates radiation and reflects it out from the beamline. The backward-generated radiation, passing through a quartz window, is collected and collimated by a 90° off-axis parabolic mirror with a focal length of 152 mm (Edmund Optics, Barrington, NJ, USA) and carried to the experimental table by a flat mirror. The coherent radiation spectrum is measured using a hand-built Michelson interferometer with a 24 µm Mylar pellicle beamsplitter coupled with a room-temperature pyroelectric detector. The transverse spatial distribution of CTR has been observed by means of a THz camera (Spiricon Camera III, Ophir, North Logan, UT, USA) placed in the focal plane of an off axis parabolic mirror (APM2) with a focal length of 50 mm (Edmund Optics, Barrington, NJ, USA). The THz total energy per pulse was measured by a second pyroelectric detector (THz-I-BNC, GENTEC-EO, Suite Quebec, Canada) with a sensitivity calibrated with 970 GHz through a Schottky Diode (Virginia Diodes Inc, Charlottesville, VA, USA) emitting a power of 1 mW. THz filters (0.3, 0.5, 1, 3 and 5 THz) , with approximately a 15% bandwidth, have been used to select different frequencies.

Narrow spectral bandwidth and tunable THz radiation can be produced by a train of sub-ps electron bunches. An active method for tailoring an adjustable train of electron bunches with a sub-picosecond length and picosecond spacing has been demonstrated at the SPARC_LAB test facility [12,23], combining the velocity bunching regime, and properly shaped trains of UV laser pulses hitting the photocathode (comb laser beam).

The technique used to generate laser comb pulses relies on a birefringent crystal, where the input pulse is decomposed in two orthogonally polarized pulses with a time separation proportional to the crystal length. If more birefringent crystals are inserted in the laser beam path, it is possible to produce multi-peaks. A comb laser pulse illuminating a metallic photocathode in a RF gun generates a train of short electron bunches. Downstream the photoinjector, the beam acquires an energy modulation because of the space charge forces and, if injected in a RF-compressor operating in the over-compression regime, the energy modulation can be transformed back into a density modulation. The train parameters, *i.e.*, bunch charge, length, and inter-distance, can be completely controlled by proper adjustment of both laser and linac settings [24]. As a train of sub-ps relativistic electron bunches crosses an aluminum screen, see Figure 2b, coherent THz radiation is generated and its spectrum results in a series of narrow pulses whose THz central frequency and bandwidth depend on the bunches inter-distance and width.

4. Results and Discussion

4.1. Broadband Generation

A broadband THz radiation spectrum has been obtained by sub-ps single bunches. In particular the Figure 3a shows the CTR spectrum for a 500 pC, 180 fs electron beam measured sampling with different band pass filters. As previously discussed, the drop below 0.3 THz is due to the effect of finite screen size combined with the fall of responsivity of pyroelectric detector. At high frequency instead the longitudinal extension of the bunch limits the generation just above 5 THz. The integrated energy per pulse reaches up to 35 μJ measured by pyroelectric detector. The Figure 3b shows the CTR spatial distribution at the corresponding frequencies, as collected and focalized by APM2. As one can see, generated CTR shows the peculiar anular distribution of radially polarized light. The spot size strongly reduces increasing the frequency due to the reduction of the source size, whose radius depends on the wavelength. In particular at 1 THz the FWHM diameter is ∼1.5 mm that correspond to a THz fluence of ∼1 mJ/cm^2.

As one observes from Equation (3), the emitted THz energy depends on the square of the bunch charge Q. Figure 4 shows the measured CTR spectra for different bunch charges, keeping the bunch length constant, as indicated by the high frequency cut-off. The detector response, the z-cut quartz window transmission and the single particle TR spectrum for a finite size target have been taken into account to retrieve the CTR spectra depicted in Figure 4. The generated THz energy is consistent with a quadratic Q^2 dependence as reported in the inset of Figure 4.

Figure 4 shows also the capability of our detecting system to measure very low charge beams, few tens of pC and less when the air-drying system is turned off. By decreasing the charge of a factor ∼45 (from 500 pC down to 11 pC), the measured pulse energy reduced from 40 μJ to 20 nJ. The low frequency components (below 0.7 THz) are not shown in Figure 4 because they are strongly affected the transmission function of Michelson interferometer (in particular Fabry-Perot interferences in Mylar BS), both diffraction limited size and drop of efficiency of pyroelectric detector. For this, such effects in particular in the low THz frequency region are difficult to evaluate and compensate.

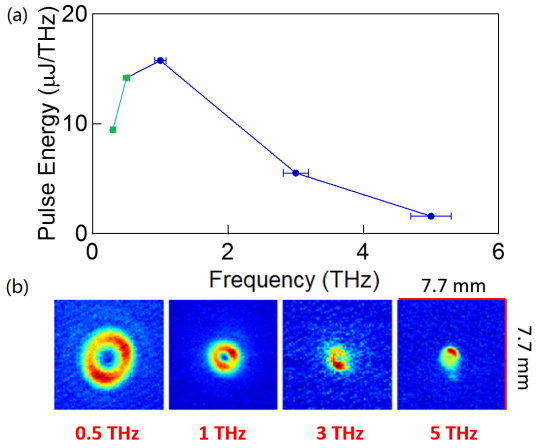

Figure 3. Broadband THz generation: (**a**) spectral distribution sampled by THz filters. The error bars represent the bandwidth of the bandpass filters; (**b**) Transverse intensity distributions of CTR in the focus of the parabolic mirror for different wavelength. Since the used power meter (THz-I-BNC GENTEC-EO) is not calibrated for frequencies below 0.61 THz, the measured energy for frequencies below this value is a qualitative assessment.

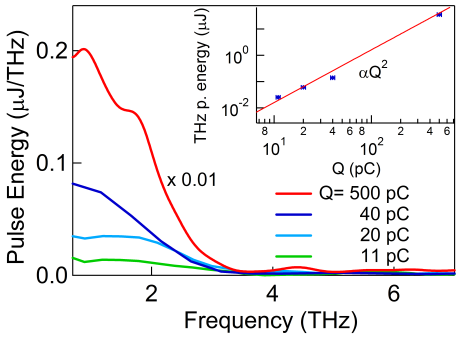

Figure 4. Low charge regime: Spectral distribution intensity measured by Michelson interferometer for different bunch charge Q. Inset: generated THz energy per pulse as a function of bunch charge Q. The curve for the highest bunch charge (500 pC) has been scaled by a factor of 100. Experimental data (blue dots), Q^2 dependence (red line). The integrated THz intensities per pulse shown in the inset are affected by a systematic uncertainty due to the missing calibration of the THz-I-BNC GENTEC-EO pyroelectric detector at low frequencies (below 0.6 THz).

4.2. Spectral-Shaped THz Generation

High charged trains of sub-ps bunches with THz repetition rate have been successfully manipulated and transported down to the linac exit to reach the THz station.

We report the characterization of THz spectral shapes generated from different configurations of 5-bunch trains, in particular the inter-distance and the bunch charge balanced by UV laser shaping.

The first studied bunch consists of a four bunches beam, each with a mean charge of ∼50 pC and an inter-distance of 1 ps. This train is followed by a further bunch with charge of ∼20 pC, which has an inter-distance of 1.6 ps from the fourth. The longitudinal phase space (time-energy) was measured by combining the RFD and the dipole spectrometer. The average energy of the whole train is ∼110 MeV with an energy spread of 0.2%. The bunch train current is reported in the inset of the Figure 5, where each bunch in the train has been labeled (1–5), while the measured beam parameters are reported in Table 1.

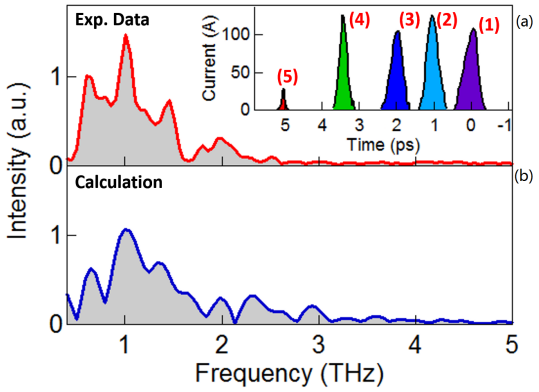

Figure 5. THz generation via Coherent Transition Radiation (CTR) by a five comb beam: (**a**) Experimental data (**b**) Numerical calculation from measured current distribution reported in the inset.

Table 1. Electron beam parameters for the three different configurations of the five bunches.

	Comb Beam 1 Inter-Distance (4)-(5) = 1.6 ps			**Comb Beam 2 Inter-Distance (4)-(5) = 0.5 ps**			**Ramp of Charge**		
	Bunch Lenght (ps)	**Position (ps)**	**Charge (pC)**	**Bunch Lenght (ps)**	**Position (ps)**	**Charge (pC)**	**Bunch Lenght (ps)**	**Position (ps)**	**Charge (pC)**
Beam 1	0.38	0	60	0.38	0	55	0.37	0	14
Beam 2	0.32	0.95	55	0.32	1.1	55	0.56	0.9	36
Beam 3	0.29	1.88	50	0.20	2.1	48	0.48	1.7	61
Beam 4	0.20	3.5	50	0.23	3.6	46	0.40	3.0	85
Beam 5	0.16	5.1	23	0.29	4.1	18	0.27	4.6	23

The generated spectral distribution measured by means of a Michelson interferometer is reported in Figure 5a. As previously discussed, respect to a gaussian-like shape emitted by a single bunch, a comb-like beam generates a peaked THz spectrum.

The central frequency of the main peaks corresponds to the inverse of the inter-distance between the bunches: the 1 THz peak is related to the mean inter-distance of ∼1 ps of the first 3 bunches, while the low frequency peak at 0.6 THz is due to the inter-distance of 1.6 ps between the last two bunches. The remaining components of the high frequency in the spectrum result from the harmonics properly enveloped by the single bunch spectrum as observed in Figure 1. Figure 5b shows the expected, calculated THz spectral emission for the measured bunch train distribution reported in the inset of Figure 5a. As one observes, the spectral calculation reproduces well the measured one.

The reduction of the inter-distance between the bunches leads to a displacement of the THz spectrum towards high frequencies, as one can see in Figure 6a. The considered bunch train is approximately identical to the previous one, as shown by the beam parameters in Table 1, but the inter-distance between the last two bunches is reduced from 1.6 ps to 0.5 ps. A narrower peak emerges in the measured THz spectrum at about 2 THz decreasing the contribution at 0.6 THz as shown by green arrows in Figure 6a. While the remaining part of the spectrum results exactly unchanged.

Also the numerical calculation of the generated spectrum, blue line in Figure 1, evaluated from measured current profile shows the rise of a narrow peak around 2 THz while the contribution at 0.6 THz decreases.

In order to investigate the production of narrow-band THz radiation, a train of four bunches with a ramp of charge has been generated directly at the cathode. The resulting electron bunch train, as measured at the end of the linac, is shown in the inset of Figure 7, while beam parameters are reported in Table 1 (third column). The generated THz spectrum, shown in Figure 7a by the red curves, has a narrow peak centered at 0.65 THz with a 20% of bandwidth respect to uniform comb beam.

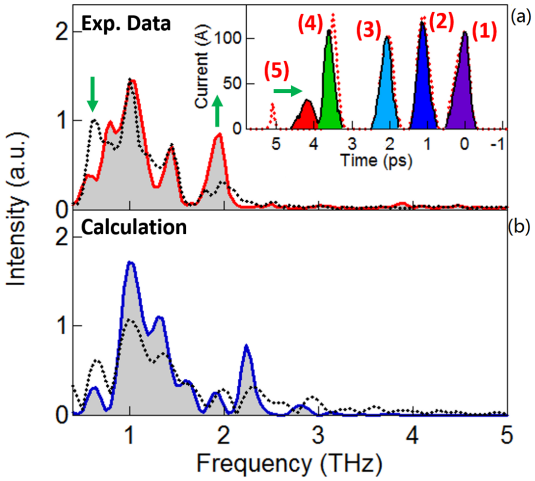

Figure 6. THz generation by a five comb beam reducing the inter-distance of the last two bunches from 1.6 ps to 0.6 ps. (**a**) Measured spectrum is shown through red curve is compared to that obtained with 1.6 ps of inter-distance (black dotted curves); (**b**) Numerical calculation from measured current distributions reported in the inset: inter-distance 0.5 ps (blue curve) and inter-distance 1.6 ps (black dotted curve).

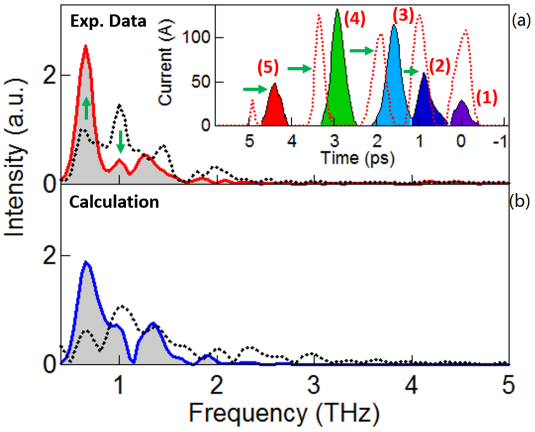

Figure 7. Narrowband generation from a ramped comb beam: (**a**) Measured THz spectrum (red line), compared to that generated from uniform beam (black dotted line); (**b**) Calculated THz spectrum from measured current distributions report in the inset: ramped (blue curve) and uniform (black dotted curve). Inset: measured ramped current distribution compared to the uniform one (red dotted line) previously discussed.

5. Figures of Merit

THz generation can be tuned by fully controlling the accelerators parameters and UV laser shape. Single sub-ps electron bunch generated by UV single pulse is used to generate highly intense and broadband THz radiation by means of RF compression (velocity bunching). Properly shaping the UV laser longitudinal distribution the THz spectral shape can be controlled, in particular a properly shaped bunch train can be used to drive narrowband THz radiation. In Table 2, the main figure of merits of the SPARC_LAB source for a single-bunch to generate broadband THz radiation and five-ramped comb train to generate a narrowband THz radiation are reported.

Table 2. SPARC_LAB THz sources: radiation and electron beam parameters for a single bunch and a ramped five-bunches train.

THz Radiation Parameters				Electron Beam Parameters	
	Single Bunch	**Ramped Comb**		**Single Bunch**	**Ramped Comb**
Energy per pulse (μJ)	35 †	∼1	Charge (pC)	500	220
Peak power (MW)	0.17 †	0.25	Energy (MeV)	121	110
Electric field (MV/cm)	>1 †	-	Bunch duration (fs)	180	130
Bandwidth (THz) $\Delta\nu$	>5	0.25	Rep. Rate (Hz)	10	10
Pulse duration t_p (ps)	<0.1	>1.8 ∗	Comb distance (ps)	-	1.3

∗ From transform-limited relationship: $\Delta\nu$ t_p = 0.44; † Systematic uncertainity due to missing detector calibration below 0.61 THz.

6. Conclusions

The SPARC_LAB test facility is actually hosting different linac-based radiation sources, e.g., a FEL source, an advanced THz source, a *X*-ray Thomson source.

In this paper, the recent results of SPARC_LAB terahertz source have been reported. A THz emission can be achieved in different regimes, controlling the bunch shaping, charge filling and bunch separation by properly set the UV photocathode laser and the linac parameters. Two main production schemes are currently investigated, ultrashort single bunch and multi-bunches electron comb beams. These schemes provide high energy per pulse and broad and narrow spectral bandwidth THz radiation, respectively. The SPARC_LAB THz source in its different potentialities is currently used for nonlinear and pump-probe experiments in Solid-State Physics and Material Science.

Acknowledgments: This work profited from the discussion and the help of the whole SPARC_LAB collaboration.

Author Contributions: F. G., E. C., M. D., S. L., M. P. and V. S. carried out the terahertz experiments. F. G., E. C. and S. L. analyzed the data and performed numerical calculations. M. P. A., M. B., A. B., E. C., A. C., M. D. F., D. D. G., F. G., G. D. P., M. F., A. M., S. P., R. P., C. V. and F. V. managed the SPARC machine and the photocathode laser during the THz measurements. F. G., E. C. and S. L. wrote the manuscript. All authors extensively discussed the results.

Conflicts of Interest: The authors declare no conflict of interest.

References

1. Wu, Z.; Fisher, A.S. Intense terahertz pulses from SLAC electron beams using coherent transition radiation. *Rev. Sci. Instr.* **2013**, *84*, doi:10.1063/1.4790427.
2. Stojanovic, N.; Drescher, M. Accelerator- and laser-based sources of high-field terahertz pulses. *J. Phys. B: Atomic Mol. Opt. Phys.* **2013**, *46*, doi:10.1088/0953-4075/46/19/192001.
3. Lee, Y.R. *Principles of Terahertz Science and Technology*; Springer Science + Business Media LLC: New York, NY, USA, 2009; pp. 59–74.
4. Zhu, B.; Chen, Y.; Deng, K.; Hu, W.; Yao, Z.S. Terahertz science and technology and applications. In Proceedings of the Progress in Electromagnetics Research Symposium, Beijing, China, 23–27 March 2009; pp. 1166–1170.
5. Yeh, K.L.; Hoffmann, M.C.; Hebling, J.; Nelson, K.A. Generation of 10 μJ ultrashort terahertz pulses by optical rectification. *Appl. Phys. Lett.* **2007**, *90*, doi:10.1063/1.2734374.
6. Vicario, C.; Monoszlai, B.; Hauri, C.P. GV/m single-cycle terahertz fields from a laser-driven large-size partitioned organic crystal. *Phys. Rev. Lett.* **2014**, *112*, doi:10.1103/PhysRevLett.112.213901.
7. Ferrario, M.; Alesini, D.; Anania, M.; Bacci, A.; Bellaveglia, M.; Bogdanov, O.; Boni, R.; Castellano, M.; Chiadroni, E.; Cianchi, A.; *et al*. SPARC_LAB present and future. *Nucl. Instrum. Methods Phys. Res. B* **2013**, *309*, 183–188.

8. Chiadroni, E.; Bacci, A.; Bellaveglia, M.; Boscolo, M.; Castellano, M.; Cultrera, L.; di Pirro, G.; Ferrario, M.; Ficcadenti, L.; Filippetto, D.; *et al*. The SPARC linear accelerator based terahertz source. *Appl. Phys. Lett.* **2013**, *102*, doi:10.1063/1.4794014.
9. Serafini, L.; Ferrario, M. Velocity bunching in photo-injectors. *AIP Conf. Proc.* **2001**, *581*, doi:10.1063/1.1401564.
10. Ferrario, M.; Alesini, D.; Bacci, A.; Bellaveglia, M.; Boni, R.; Boscolo, M.; Castellano, M.; Chiadroni, E.; Cianchi, A.; Cultrera, L.; *et al*. Experimental Demonstration of Emittance Compensation with Velocity Bunching. *Phys. Rev. Lett.* **2010**, *104*, doi:10.1103/PhysRevLett.104.054801.
11. Ferrario, M.; Alesini, D.; Bacci, A.; Bellaveglia, M.; Boni, R.; Boscolo, M.; Castellano, M.; Chiadroni, E.; Cianchi, A.; Cultrera, L.; *et al*. Laser comb with velocity bunching: Preliminary results at SPARC. *Nucl. Instr. Methods Phys. Res. Sect. A: Accel. Spectrom. Detect. Assoc. Equip.* **2011**, *637*, S43–S46.
12. Chiadroni, E.; Bellaveglia, M.; Calvani, P.; Castellano, M.; Catani, L.; Cianchi, A.; di Pirro, G.; Ferrario, M.; Gatti, G.; Lupi, S.; *et al*. Characterization of the THz radiation source at the Frascati linear accelerator. *Rev. Sci. Instrum.* **2013**, *84*, doi:10.1063/1.4790429.
13. Gensch, M.; Bittner, L.; Chesnov, A.; Delsim-Hashemi, H.; Drescher, M.; Faatz, B.; Feldhaus, J.; Fruehling, U.; Geloni, G.A.; Gerth, Ch.; *et al*. New infrared undulator beamline at FLASH. *Infrared Phys. Technol.* **2008**, *51*, 423–425.
14. Cook, A.M.; Tikhoplav, R.; Tochitsky, S.Y.; Travish, G.; Williams, O.B.; Rosenzweig, J.B. Observation of Narrow-Band Terahertz Coherent Cherenkov Radiation from a Cylindrical Dielectric-Lined Waveguide. *Phys. Rev. Lett.* **2011**, *103*, doi:10.1103/PhysRevLett.103.095003.
15. Shen, Y.; Yang, X.; Garr, G.L.; Hidaka, Y.; Murphy, J.B.; Wang, X. Tunable Few-Cycle and Multicycle Coherent Terahertz Radiation from Relativistic Electrons. *Phys. Rev. Lett.* **2011**, *107*, doi:10.1103/PhysRevLett.107.204801.
16. Muggli, P.; Yakimenko, V.; Babzien, M.; Kallos, E.; Kusche, K.P. Generation of Trains of Electron Microbunches with Adjustable Subpicosecond Spacing. *Phys. Rev. Lett.* **2011**, *101*, doi:10.1103/PhysRevLett.101.054801.
17. Perucchi, A.; Baldassarre, L.; Postorino, P.; Lupi, S. Optical properties across the insulator to metal transitions in vanadium oxide compounds. *J. Phys. Condensed Matter* **2009**, *21*, doi:10.1088/0953-8984/21/32/323202.
18. Calvani, P.; Capizzi, M.; Lupi, S.; Balestrino, G. Infrared active vibrational modes strongly coupled to carriers in high-Tc superconductors. *Europhys. Lett.* **1995**, *31*, 473–478.
19. Ferrario, M.; Alesini, D.; Alessandroni, M.; Anania, M.P.; Andreas, S.; Angelone, M.; Arcovito, A.; Arnesano, F.; Artioli, M.; Avaldi, L.; *et al*. IRIDE: Interdisciplinary research infrastructure based on dual electron linacs and lasers. *Nuc. Instr. Methods Phys. Res. Sect. A: Accel. Spectrom. Detect. Assoc. Equip.* **2014**, *740*, 138–146.
20. Rossi, A.R.; Bacci, A.; Belleveglia, M; Chiadroni, E.; Cianchi, C.; di Pirro, G.; Ferrario, M.; Gallo, A.; Gatti, G.; Maroli, C.; *et al*. The External-Injection experiment at the SPARC_LAB facility. *Nucl. Instrum. Methods Phys. Res. Sect. A: Accel. Spectrom. Detect. Assoc. Equip.* **2014**, *740*, 60–66.
21. Landau, L.D.; Lifschitz, E.M. *Electrodynamics of Continuous Media*; Pergamon Press Ltd.: Oxford, UK, 1984; pp. 410–412.
22. Castellano, M.; Cianchi, A.; Orlandi, G.; Verzilov, V.A. Effect of diffraction and target finite size on coherent transition radiation spectra in bunch length measurement. *Nucl. Instrum. Methods Phys. Res. A* **1999**, *435*, 297–307.
23. Marchetti, B.; Bacci, A.; Chiadroni, E.; Cianchi, A.; Ferrario, M.; Mostacci, A.; Pompili, R.; Ronsivalle, C.; Spataro, B.; Zagorodnov, I. Novel schemes for the optimization of the SPARC narrow band THz source. *Rev. Sci. Instrum.* **2015**, *86*, doi:10.1063/1.4922882.
24. Mostacci, A.; Alesini, D.; Antici, P.; Bacci, A.; Bellaveglia, M.; Boni, R.; Castellano, M.; Chiadroni, E.; Cianchi, A.; di Pirro, G.; *et al.* Advanced beam manipulation techniques at SPARC. In Proceedings of the IPAC2011, THYB01, San Sebastn, Spain, 4 September 2011.